JOURNAL OF COMPUTATIONAL PHYSICS 116, 262–276 (1995)

Velocity Boundary Conditions for the Simulation of Free Surface Fluid Flow

SHEA CHEN, DAVID B. JOHNSON, AND PETER E. RAAD

Mechanical Engineering Department, Southern Methodist University, Dallas, Texas 75275-0337

Received June 25, 1992; revised June 27, 1994

Accurate velocity boundary conditions are critical to the successful simulation of free surface fluid flow. It is shown in this paper that previous approaches for the assignment of free surface velocity boundary conditions in marker and cell methods artificially introduce asymmetry and can even cause the simulation to break up. New approaches are presented that improve the accuracy of the treatment of free surface velocity boundary conditions. The significant advantages of the use of these new approaches are demonstrated by simulation results obtained for broken dam and cavity filling problems. The new approaches do not artificially introduce asymmetry. Although symmetry is a useful, tangible indicator, it is shown that the significance of the new approaches extends beyond the elimination of asymmetry. Their use enables the successful simulation of problems with realistic values of viscosity and gravity, problems for which breakup of the solution occurs if previous approaches are employed.

1. INTRODUCTION

The finite difference simulation of transient, incompressible, free surface fluid flow presents unique challenges. Two of these challenges are that the location of the free surface itself is unknown and that no equation that describes changes of pressure with time is available. In 1965, these challenges were first addressed in the marker and cell (MAC) method by Harlow and Welch [9] and Welch, Harlow, Shannon, and Daly [25]. They introduced massless markers that move with the fluid and a novel finite difference solution algorithm for the velocity field. The massless markers are used to define the location and track the movement of the free surface. Several authors have presented extensions and modifications of the MAC method [10, 13, 15, 20, 23, 24]. Hirt and Shannon [14] and Nichols and Hirt [19] addressed the free surface stress conditions. Chan, Street, and Fromm [6, 7] published the SUMMAC method for plane wave problems, which introduced the extrapolation of velocity components from the fluid interior to obtain velocity boundary conditions. Another approach to the simulation of single-valued free surface fluid flow problems, the height function method, was described by Bulgarelli, Casulli, and Greenspan [5], Lardner and Song [16], and Loh and Rasmussen [17]. Hirt, Cook, and Butler [11] presented a Lagrangian technique for flows that do not undergo large distortions. Amsden and Harlow [2, 3] introduced the simplified marker and cell (SMAC) method. Amsden [1] modified the SMAC method to incorporate the use of surface markers and line segments for single-valued free surfaces; Nakayama and Romero [18] extended the application of the SMAC method to fluid flows that are almost three-dimensional. Chen, Johnson, and Raad [8] introduced the surface marker (SM) method, which represents a modification of the SMAC method to incorporate the use of surface markers. The SM method does not make use of line segments and is not limited to the simulation of problems with single-valued free surfaces. In the SM method, new marker treatment and cell reflagging techniques are introduced that result in significant reductions of the computer time and memory requirements. In other respects, the SM method is identical to the SMAC method. The methods associated with all of the preceding extensions and modifications, while distinct, all employ massless markers and a staggered grid of finite difference cells and are hereafter referred to generically as marker and cell methods. A finite difference method for the simulation of free surface fluid flow problems based on the concept of a fractional volume of fluid (VOF) rather than on the use of massless markers was developed by Hirt and Nichols [12]; Nichols, Hirt, and Hotchkiss [21]; Torrey, Cloutman, Mjolsness, and Hirt [22]; and Ashgriz and Poo [4]. The emphasis in this paper is on marker and cell methods.

For any free surface fluid flow simulation method, the treatment of the velocity boundary conditions associated with the free surface has a crucial impact on the simulation. Because of their importance to the simulation of free surface fluid flow, the focus of the present paper is on the treatment of velocity boundary conditions. In particular, the emphasis is on the treatment of the velocity boundary conditions in connection with the use of a marker and cell method. As the solution progresses, velocity boundary conditions are required for the determination of the fluid velocity field as well as for the movement of the markers that define the location of the free surface.

In the next section, the basic computational cycle associated with the predictor–corrector solution algorithm introduced by Amsden and Harlow [2] is outlined, and the steps in the computational cycle in which velocity boundary conditions are required are noted. Then, the three different types of velocity

0021-9991/95 $6.00

boundary conditions are defined, and new methods for determining surface, just outside tangential, and new internal velocities are presented. Differences, as well as similarities, between the new methods presented in this paper and the MAC and SMAC approaches are noted. The height function method and the extrapolation approach introduced in the SUMMAC method, however, are not discussed since both methods are limited to plane wave problems. Although the VOF method is not a marker and cell method, it is worth noting that surface and just outside tangential velocities are computed by use of the MAC schemes in the VOF method, while new internal velocities are estimated by use of the volume of fluid function. In Section 6, the advantages of the use of the proposed velocity boundary conditions are demonstrated by specific numerical examples.

2. THE COMPUTATIONAL CYCLE

One computational cycle in the simulation of unsteady free surface fluid flow consists of the advancement of the discrete field variables from an initial time t_0 to the subsequent time $t_0 + \delta t$ by accomplishing the seven steps listed below. The first four steps represent a predictor–corrector algorithm for the determination of the velocity field at $t_0 + \delta t$. In the predictor stage of the solution algorithm, the pressure is replaced by an arbitrary pseudopressure θ, and tentative velocities are then calculated. Since the authors of SMAC [2] state (1) that the pseudopressure field θ can *only* affect the solution efficiency of the Poisson equation, (2) that θ *generally* is set equal to zero, and (3) that θ in some cases *must* be set equal to zero, we have decided to choose $\theta = 0$ always in full cells. A pseudopressure boundary condition is applied in surface cells to satisfy the normal stress condition. Since pressure has been ignored (or assigned an arbitrary value) in the full cells, the tentative velocity field does not satisfy the incompressible continuity equation. The deviation from incompressibility is used to calculate a pressure potential[1] field ψ, which then is used to correct the velocity field. In the final three steps, the velocity boundary conditions are calculated, the new location of the free surface is determined, and the velocity boundary conditions associated with new fluid cells are assigned:

1. Compute a tentative velocity field, $\tilde{u}$ and $\tilde{v}$, at $t_0 + \delta t$ from the preceding velocity field by the use of

$$\frac{\partial \tilde{u}}{\partial t} = -\frac{\partial u^2}{\partial x} - \frac{\partial uv}{\partial y} + \nu\left(\frac{\partial^2 u}{\partial x^2} + \frac{\partial^2 u}{\partial y^2}\right) - \frac{\partial \theta}{\partial x} + g_x$$

and (1)

$$\frac{\partial \tilde{v}}{\partial t} = -\frac{\partial v^2}{\partial y} - \frac{\partial uv}{\partial x} + \nu\left(\frac{\partial^2 v}{\partial x^2} + \frac{\partial^2 v}{\partial y^2}\right) - \frac{\partial \theta}{\partial y} + g_y,$$

where u and v are the x- and y-components of the fluid velocity; g_x and g_y represent the x- and y-components of gravity, respectively; θ is the pseudopressure; and ν is the kinematic viscosity of the fluid.

2. Calculate the incompressibility deviation function D defined by

$$D = \frac{\partial \tilde{u}}{\partial x} + \frac{\partial \tilde{v}}{\partial y}. \tag{2}$$

3. Solve for the pressure potential field ψ by use of the Poisson equation

$$\frac{\partial^2 \psi}{\partial x^2} + \frac{\partial^2 \psi}{\partial y^2} = D. \tag{3}$$

4. Compute the corrected velocity components at $t_0 + \delta t$ by use of

$$u = \tilde{u} - \frac{\partial \psi}{\partial x}, \quad v = \tilde{v} - \frac{\partial \psi}{\partial y}. \tag{4}$$

5. Adjust the surface velocity and just outside tangential velocity boundary conditions.

6. Track the movement and define the new location of the fluid free surface.

7. Determine the velocity boundary conditions required in the next calculational cycle.

The focus of this paper is on the algorithms required in Steps 5 and 7 of the computational cycle for the determination of velocity boundary conditions. The algorithms employed in Steps 5 and 7 to determine the velocity boundary conditions are independent of the mathematical techniques used in Steps 1 through 4 in connection with Eqs. (1)–(4). In order to discuss these velocity boundary conditions in detail, it is first necessary to describe the computational mesh.

In marker and cell methods, the staggered grid concept is employed to locate the discrete field variables; and three different control volumes, one for x-momentum, one for y-momentum, and one for mass conservation, are employed [9]. The momentum control volumes are not discussed in this paper. The mass conservation control volume, which coincides with the computational cell, is of primary interest for the application of free surface velocity boundary conditions.

[1] In SMAC [2], three symbols ϕ, θ, and ψ are used that are related to pressure. The symbol ϕ is referred to as the "true pressure" and is equal to the pressure divided by the density; the symbol θ is referred to as the "pseudopressure," and ψ is simply referred to as a "potential." The relationship between ϕ, θ, and ψ is $\phi = \theta + \psi/\delta t$, which is found on page 5 of Ref. [2]. In other words, this equation states that the true pressure is the sum of the pseudopressure and the potential divided by a time increment. The pressure potential ψ that we refer to is precisely the potential ψ that is referred to in Ref. [2].

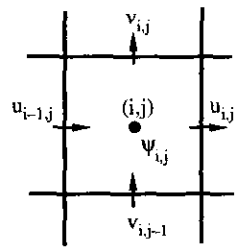

FIG. 1. Staggered grid locations of field variables for cell (i, j).

For cell (i, j), as shown in Fig. 1, the discrete velocities $u_{i,j}$, $v_{i,j}$, $u_{i-1,j}$, and $v_{i,j-1}$, are located at the mid-points of the faces of the cell; while the pressure potential $\psi_{i,j}$ is located at the center of the cell. Each cell within the computational domain is flagged at each discrete value of time as one of four types: empty, surface, full, or obstacle. In figures, these cells are identified in shorthand notation as EMP, SUR, FUL, and OB, respectively. An empty cell has no fluid in it; a surface cell contains fluid and is adjacent to an empty cell; a full cell contains fluid and has no empty neighbors; and an obstacle cell defines the location of a rigid, stationary obstacle. In this paper, velocities that are tentatively updated by use of Eqs. (1) and then corrected by use of Eqs. (4) are referred to as internal velocities. A velocity that must be determined by any other means is referred to as a velocity boundary condition.

There are three distinct types of velocity boundary conditions: new fluid cell internal velocities, surface velocities, and just outside tangential velocities. The surface and just outside tangential velocities can be thought of as the free surface normal and tangential velocity boundary conditions, respectively. On the other hand, the new fluid cell internal velocities are not free surface velocity boundary conditions at all. They are, however, created by the advancement of the free surface and must be initialized before they can be tentatively computed by use of Eqs. (1) and corrected by use of Eqs. (4) in the next computational cycle.

In each of the next three sections, one of the three distinct types of velocity boundary conditions is defined; the previous approaches for the determination of boundary conditions of that type are described; and a new approach for the determination of boundary conditions of that type is presented. New fluid cell internal velocities are discussed first, followed by surface velocities and then just outside tangential velocities.

3. NEW FLUID CELL INTERNAL VELOCITIES

New fluid cells are created during a computational cycle by the movement of markers into cells that did not contain markers at the start of the cycle. The internal velocities between new fluid cells are unknown and must be assigned. In our new approach, each unknown new fluid cell internal velocity is assigned either the value of the closest known surface or internal velocity, or the average of two neighboring surface and/or internal velocities. The basic idea behind our new approach is that the most appropriate available velocity information in the neighborhood of the unknown new fluid cell internal velocity should be used. The most appropriate velocity information is that which captures the momentum history of the fluid that has entered the new fluid cell. The information must be used in such a way that no artificial asymmetry is introduced by the velocity assignment scheme itself, as is the case for both the MAC and SMAC velocity assignment schemes. The specific details of the implementation of the new method are described with reference to Fig. 2.

3.1. *The New Procedure*

In Fig. 2, cell (i, j) represents a new fluid cell that has been created during the current computational cycle as a result of marker movement, and $u_{i,j}$ is an unknown new internal velocity. In the new method, the following hierarchical procedure is used to assign a value to $u_{i,j}$:

(a) If both $u_{i,j+1}$ and $u_{i,j-1}$ were known surface or internal velocities at $t = t_0$, then

$$u_{i,j} = (u_{i,j+1} + u_{i,j-1})/2.$$

(b) Otherwise, if $u_{i,j+1}$ was a known surface or internal velocity at $t = t_0$, then

$$u_{i,j} = u_{i,j+1}.$$

(c) Otherwise, if $u_{i,j-1}$ was a known surface or internal velocity at $t = t_0$, then

$$u_{i,j} = u_{i,j-1}.$$

(d) Otherwise, both $u_{i-1,j}$ and $u_{i+1,j}$ were known surface velocities at $t = t_0$, and

$$u_{i,j} = (u_{i-1,j} + u_{i+1,j})/2.$$

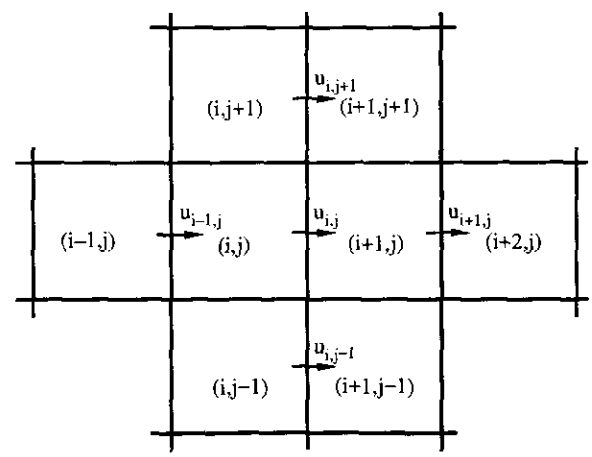

FIG. 2. *New fluid cell internal velocity* $u_{i,j}$.

This hierarchical procedure is based on the following considerations: Cells (i, j) and $(i + 1, j)$ both were empty cells at the start of the computational cycle. Since the time step is such that no marker can move during one cycle a distance as large as the cell spacing, it is not possible for a marker to have moved during the current cycle from either cell $(i - 1, j)$ or $(i + 2, j)$ to the face on which $u_{i,j}$ is located. Therefore, any fluid that has reached this face can only have come from cells $(i, j - 1)$, $(i, j + 1)$, $(i + 1, j - 1)$, and/or $(i + 1, j + 1)$. Consequently, $u_{i,j+1}$ and $u_{i,j-1}$ are the candidate neighboring fluid velocities for use in the assignment of the new fluid cell internal velocity $u_{i,j}$. If both $u_{i,j+1}$ and $u_{i,j-1}$ are available, they are averaged as indicated in case (a). If only one is available, it is used as indicated in cases (b) and (c). If neither $u_{i,j+1}$ nor $u_{i,j-1}$ is available, then all four cells $(i, j - 1)$, $(i, j + 1)$, $(i + 1, j - 1)$, and $(i + 1, j + 1)$ also were empty cells at the start of the computational cycle. In this case, the only possibility that can result in $u_{i,j}$ becoming a new fluid cell internal velocity is that both of cells $(i - 1, j)$ and $(i + 2, j)$ contained free surfaces that were moving toward each other at the start of the computational cycle. In this situation, $u_{i,j}$ is set equal to the average of $u_{i-1,j}$ and $u_{i+1,j}$ as indicated in case (d).

The new procedure for the assignment of unknown new fluid cell internal velocities makes use of the most appropriate available velocity information, while simultaneously avoiding the artificial introduction of asymmetry. Alternative procedures are employed in the MAC and SMAC methods for utilizing the available velocity information to assign a value to an unknown new fluid cell internal velocity. In contrast to the new procedure, the MAC and SMAC procedures both artificially introduce asymmetry, a fact that has not been reported previously in the literature. The details of the use of the new procedure in connection with a specific example are presented in the following. For comparison, the details of the use of the MAC and SMAC procedures also are provided.

3.2. *A Detailed Example*

Several cells on the left and right sides of the axis of symmetry of a symmetrical free surface fluid flow problem are displayed in Fig. 3. The general pattern of flow at the instant under consideration is up and toward the axis of symmetry. To facilitate the discussion, two horizontal grid lines are designated by J and $J - 1$; two vertical grid lines on the left are designated by L and $L + 1$; and two vertical grid lines on the right are designated by R and $R + 1$. Grid lines L and R are equidistant from the axis of symmetry. The locations of the free surface before and after marker movement are indicated by solid and dashed lines, respectively. Six markers $l_1, l_2, ..., l_6$ are displayed in the left half of the figure, and six markers, $r_1, r_2, ..., r_6$ are displayed in the right half. Arrows indicate the changes in the positions of the markers that occur during marker movement. The solution is assumed to be perfectly symmetrical prior to marker movement. Therefore, $u(l_i) = -u(r_i)$ for $i = 1, ..., 6$; where the notation $u(l_i)$ is used to indicate the x-component of the velocity of marker l_i. The velocities of the six markers $l_1, ..., l_6$ are, however, all assumed to be different. All of the cells into which the markers move were empty cells at the beginning of the computational cycle.

Following marker movement, the velocities $u(L, J)$ and $u(R, J)$ both are unknown new fluid cell internal velocities that must be assigned. The assignment of values to $u(L, J)$ and $u(R, J)$ is the focus of this example. For symmetry to be maintained, they must be assigned equal and opposite values.

For the new method, case (c) from Section 3.1 applies to this particular example, and $u(L, J)$ and $u(R, J)$ therefore are assigned according to

$$u(L, J) = u_a, \quad u(R, J) = -u_a.$$

In the new method, it is clear both that the most appropriate available information has been used and that symmetry has been maintained. The new approach is fundamentally different than the approaches used in either the MAC or SMAC methods, both of which introduce asymmetry artificially, as shown in the following.

According to the MAC method [25, p. 79], an unknown new internal velocity is assigned the average velocity of the markers that have entered one of the two new fluid cells with which the new internal velocity is associated. The result depends, therefore, on whether the cells are swept from left to right or from right to left. Regardless of the direction of cell sweeping, an asymmetric result is obtained. For the example of Fig. 3, if the direction of cell sweeping is from left to right, then the values of $u(L, J)$ and $u(R, J)$ are determined by the velocities of the markers that have entered cells (L, J) and (R, J), respectively, with the result that

$$u(L, J) = [u(l_2) + u(l_3)]/2, \quad u(R, J) = [u(r_4) + u(r_5)]/2.$$

Since $u(L, J) \neq -u(R, J)$, asymmetry is artificially introduced by the velocity assignment procedure itself. If, on the other hand, the direction of cell sweeping is from right to left, the two unknown new internal velocities are determined instead by the velocities of the markers that have entered cells $(R + 1, J)$ and $(L + 1, J)$, and the MAC velocity assignment procedure leads to

$$u(R, J) = [u(r_2) + u(r_3)]/2, \quad u(L, J) = [u(l_4) + u(l_5)]/2.$$

Once again, the values of $u(R, J)$ and $u(L, J)$ are not equal and opposite, and asymmetry is artificially introduced.

For the SMAC method [2, p. 54], the unknown new internal velocity is determined by the first marker to enter either one of the two new fluid cells associated with the unknown new internal velocity under consideration. The value assigned is that of the closest appropriate velocity associated with the cell from which that first marker came. As a consequence, the

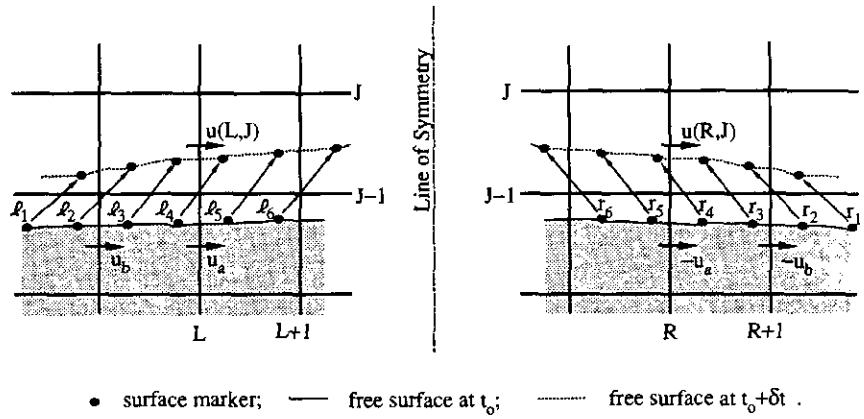

FIG. 3. New fluid cell velocities $u(L, J)$ and $u(R, J)$ in a symmetrical problem.

SMAC result depends on the order in which the markers are numbered. If the order of marker sequencing for the example in Fig. 3 is $l_1, ..., l_6, ..., r_6, ..., r_1$; then the first marker to enter cell (L, J) is l_2; and the first marker to enter cell (R, J) is r_5. Therefore, the values assigned to the unknown new internal velocities are

$$u(L, J) = u_b, \quad u(R, J) = -u_a.$$

Since u_a and u_b are not equal, it is clear that $u(L, J) \neq -u(R, J)$ and that asymmetry is also artificially introduced by the SMAC velocity assignment procedure. If the order of marker sequencing instead is $r_1, ..., r_6, ..., l_6, ..., l_1$; then the first markers to enter cells $(R + 1, J)$ and $(L + 1, J)$ are r_2 and l_5, respectively, with the result that

$$u(R, J) = -u_b, \quad u(L, J) = u_a.$$

As before, the SMAC values of the new internal velocities are not equal and opposite, and asymmetry is artificially introduced.

Examination of this example leaves no doubt that the MAC and SMAC assignment procedures for unknown new fluid cell internal velocities both artificially introduce asymmetry. The example also demonstrates clearly that the new procedure accurately utilizes the most appropriate information available and does not artificially introduce asymmetry.

4. SURFACE VELOCITIES

A velocity that is normal to a face shared by a surface cell and an empty cell is referred to as a surface velocity. Consequently, velocities $v_{i,j-1}$, $u_{i,j}$, and $u_{i,j+1}$ of Fig. 4 all are surface velocities. A given surface cell can share faces with one, two, or three empty cells, and different procedures for assigning surface velocities apply in different situations. In the following, the procedures used in the new method for treating the four possible situations are presented. The procedure used in the new method for the first situation is identical to the procedure used in previous methods for the same situation. New procedures are presented for the treatment of the other three situations.

The main consideration in each situation is the satisfaction of the continuity equation for the control volume represented by the surface cell. All surface velocities must be assigned twice during each computational cycle: first following the computation of final velocities; then again following the movement of markers and the reflagging of cells. In previous methods, the same procedures are used to assign both the final surface velocities and the new fluid cell surface velocities. In the new method presented in this paper, different procedures are used in some situations for assigning surface velocities at the two different steps in the computational cycle.

4.1. *One Empty Neighbor*

For a surface cell with one empty neighbor, the single surface velocity is assigned by use of the continuity equation. For

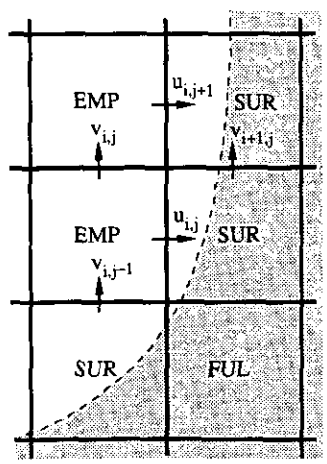

FIG. 4. Surface velocity and just outside tangential velocity boundary conditions.

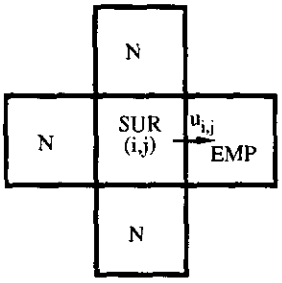

FIG. 5. A surface cell with one empty neighbor (N = non-empty).

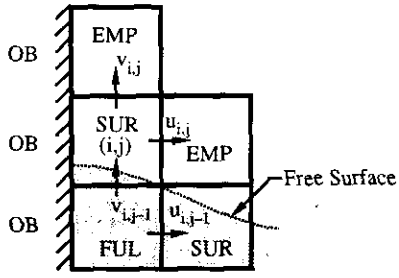

FIG. 7. A surface cell (i, j) with two adjacent empty neighbors and one obstacle neighbor.

example, the surface velocity $u_{i,j}$ in Fig. 5 is assigned according to

$$u_{i,j} = u_{i-1,j} - (v_{i,j} - v_{i,j-1})\,\delta x/\delta y, \tag{5}$$

where δx and δy represent the cell dimensions in the x- and y-directions, respectively. There is no difference between this approach and the approach used in both the MAC and SMAC methods.

4.2. *Two Adjacent Empty Neighbors*

For the situation of a surface cell that has two adjacent empty neighbors, as shown in Fig. 6, two different cases are recognized in the new method. If neither of the non-empty neighbors is an obstacle cell, the surface velocities $u_{i,j}$ and $v_{i,j}$ shown in Fig. 6 are assigned as

$$u_{i,j} = u_{i-1,j}, \quad v_{i,j} = v_{i,j-1}. \tag{6}$$

The continuity equation for cell (i, j) is clearly satisfied by these assignments. This is exactly the approach used in both the MAC and SMAC methods.

On the other hand, a new procedure is proposed when one of the non-empty neighbors is an obstacle cell, as shown in Fig. 7. This important case, one that is not recognized at all in previous methods, is not uncommon. It will occur repeatedly, for example, as fluid moves along the face of a rigid obstacle. The surface velocity assignment scheme presented above for a surface cell with two adjacent empty neighbors is entirely inappropriate in this case. The surface velocity assignment procedure for this case has a very significant influence on the simulation of the advance of a free surface along an obstacle.

For cell (i, j) of Fig. 7, the new approach is to assign to the surface velocity $u_{i,j}$ either the value of $u_{i,j-1}$, if $u_{i,j-1}$ is positive, or a zero value, if $u_{i,j-1}$ is negative or zero. Then, the other surface velocity $v_{i,j}$ is calculated to ensure that the incompressibility deviation $D_{i,j}$ vanishes. In analytical terms, the new approach is to assign the surface velocities for cell (i, j) of Fig. 7 according to

$$\begin{aligned} u_{i,j} &= \max(u_{i,j-1}, 0), \\ v_{i,j} &= v_{i,j-1} - u_{i,j}\,\delta y/\delta x. \end{aligned} \tag{7}$$

Since cell $(i - 1, j)$ is an obstacle cell, the value of $u_{i-1,j}$ is zero. Consequently, $u_{i-1,j}$ does not appear in the expression for $v_{i,j}$ in Eqs. (7).

This new approach was adopted for the following reasons. If Eq. (6) is used for the situation shown in Fig. 7, then the velocity $u_{i,j}$ is set equal to $u_{i-1,j}$, which is zero since cell $(i - 1, j)$ is an obstacle cell. As long as cell (i, j) remains a surface cell with adjacent empty neighbors, $u_{i,j}$ remains equal to zero, regardless of the value of $u_{i,j-1}$, which is the nearest fluid velocity. In this special case, the value of $u_{i-1,j}$ does not have any relation at all to the motion of the fluid that is moving up the face of the vertical obstacle. It is more accurate in this case, therefore, to assign $u_{i,j}$ the value of $u_{i,j-1}$, the nearest horizontal velocity that is related to the motion of the fluid. However, this assignment is not appropriate when $u_{i,j-1}$ is negative. If $u_{i,j-1}$ is negative, the subsequent determination of $v_{i,j}$ by use of the continuity equation results in a value of $v_{i,j}$ that is larger than $v_{i,j-1}$, and the result is that a very thin strip of fluid, much narrower than the width of a cell, moves rapidly up the face of the obstacle. Therefore, a value of zero is assigned to $u_{i,j}$ when $u_{i,j-1}$ is negative.

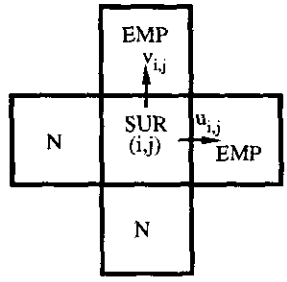

FIG. 6. A surface cell with two adjacent empty neighbors (N = non-empty).

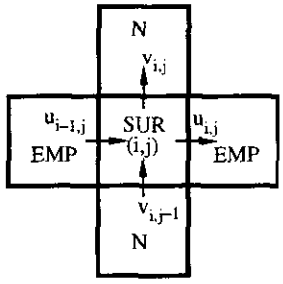

FIG. 8. A surface cell with two opposite empty neighbors (N = non-empty).

4.3. *Empty Neighbors on Opposite Sides*

An original treatment that makes use of the incompressibility deviation to compute appropriate values for the required surface velocities is presented for the case of a surface cell with empty neighbors on opposite sides. The new assignment procedure also includes a special provision that applies if the surface cell in question is a new fluid cell.

The specific situation shown in Fig. 8 is referred to in the description of the new procedure. Just prior to the assignment of the surface velocities $u_{i,j}$ and $u_{i-1,j}$, the incompressibility deviation

$$D_{i,j} = \frac{u_{i,j} - u_{i-1,j}}{\delta x} + \frac{v_{i,j} - v_{i,j-1}}{\delta y} \tag{8}$$

will, in general, not be equal to zero as a result of changes in $v_{i,j}$ and $v_{i,j-1}$. In order to ensure that $D_{i,j}$ vanishes, the surface velocities are adjusted according to

$$\begin{aligned} u_{i,j} &= u_{i,j} - D_{i,j}\,\delta x/2 \\ u_{i-1,j} &= u_{i-1,j} + D_{i,j}\,\delta x/2. \end{aligned} \tag{9}$$

Equations (8) and (9) are used to compute new surface velocities as well as final surface velocities. For a new surface cell, however, appropriate initial values of $u_{i,j}$ and $u_{i-1,j}$ first must be obtained.

The velocities $u_{i,j}$ and $u_{i-1,j}$ are unknown if cell (i, j) is a new fluid cell. Therefore, if cell (i, j) is a new fluid cell, initial values for $u_{i,j}$ and $u_{i-1,j}$ that capture the momentum history of the fluid that has entered the cell are assigned prior to the calculation of $D_{i,j}$ according to

$$\begin{aligned} u_{i,j} &= (u_{i,j+1} + u_{i,j-1})/2 \\ u_{i-1,j} &= (u_{i-1,j+1} + u_{i-1,j-1})/2. \end{aligned}$$

Then, $D_{i,j}$ is computed by use of Eq. (8), and $u_{i,j}$ and $u_{i-1,j}$ are adjusted according to Eq. (9).

The new procedure described above ensures that the continuity equation is satisfied in a surface cell with empty neighbors on opposite sides. In addition, the special case of a surface cell with empty neighbors on opposite sides that happens also to be a new fluid cell is recognized and treated. Importantly, the new procedure does not artificially introduce asymmetry.

By contrast, the MAC method does not recognize the case of a surface cell with empty neighbors on opposite faces at all, and the SMAC procedure for the assignment of surface velocities in this case artificially introduces asymmetry. This consequence of the SMAC procedure, which has not been noted previously, is demonstrated in the following example.

A situation involving two surface cells with empty neighbors on opposite faces is shown in Fig. 9. The two cells are equidistant from the axis of symmetry of a symmetrical free surface fluid flow problem. At the start of the computational cycle, it is assumed that the velocity field, including the surface velocities, is perfectly symmetrical and, in particular, that

$$\begin{aligned} u(L, J) &= -u(R, J) = u_a, \\ u(L-1, J) &= -u(R+1, J) = u_b. \end{aligned}$$

In addition, it is also assumed that the final internal velocity field also is symmetrical and, therefore, that

$$\begin{aligned} v(L, J-1) &= v(R+1, J-1), \\ v(L, J) &= v(R+1, J). \end{aligned}$$

The focus of this example is on the subsequent assignment of the surface velocities $u(L-1, J)$, $u(L, J)$, $u(R, J)$, and $u(R+1, J)$.

According to the SMAC procedure [2, p. 12], the surface velocity on the left side of the surface cell in question retains its previous value, while the surface velocity on the right side of the cell is computed by use of the continuity equation. For this example, therefore, the SMAC results are

$$\begin{aligned} u(L-1, J) &= u_b \quad \text{(retains previous value)} \\ u(L, J) &= u_b - [v(L, J) - v(L, J-1)]\,\delta y/\delta x \quad \text{(assigned)} \\ u(R, J) &= -u_a \quad \text{(retains previous value)} \\ u(R+1, J) &= -u_a - [v(R+1, J) \\ &\qquad -v(R+1, J-1)]\,\delta y/\delta x \quad \text{(assigned)}. \end{aligned}$$

Since $u(L, J) \neq -u(R, J)$ and $u(L-1, J) \neq -u(R+1, J)$, it is clear that the SMAC surface velocity assignment procedure itself has artificially introduced asymmetry.

4.4. *Three Empty Neighbors*

For a new fluid cell that also is a surface cell with three empty neighbors, an original approach is introduced. The occurrence of this situation is not uncommon in transient free surface

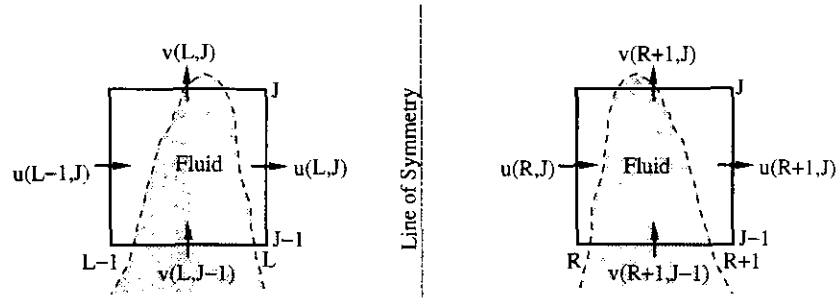

FIG. 9. Surface cells with empty neighbors on opposite sides in a symmetrical problem.

fluid flow simulations. The specific situation shown in Fig. 10b will be referred to in the description of the new approach. This situation will occur when a small amount of fluid enters cell (i, j) from below. Since the pressures in the empty cells on the left and the right of cell (i, j) are equal, the new surface velocities $u_{i,j}$ and $u_{i-1,j}$ are set equal to each other and to the average of the nearest internal velocities according to

$$u_{i,j} = u_{i-1,j} = (u_{i,j-1} + u_{i-1,j-1})/2. \tag{10}$$

The other new surface velocity $v_{i,j}$ is simply assigned the value of internal velocity $v_{i,j-1}$. With these choices, the incompressibility deviation $D_{i,j}$ vanishes. In addition, no artificial asymmetry is introduced by this new procedure.

If surface cell (i, j) is not a new fluid cell, the same procedure used in the MAC method is used in the new method. The surface velocity on the face opposite the non-empty face is assigned the value of the velocity on the non-empty face, and the values of the other two surface velocities are left unchanged. Therefore, if cell (i, j) in Fig. 10b is not a new fluid cell, $u_{i,j}$ and $u_{i-1,j}$ do not change, and $v_{i,j}$ is assigned the value of $v_{i,j-1}$. No artificial asymmetry is introduced by this procedure, and the continuity equation is satisfied for the surface cell. It is noted in passing that the SMAC procedure, on the other hand, does artificially introduce asymmetry for two of the four possible situations of a surface cell with three empty neighbors. The SMAC procedure is to assign either $u_{i,j}$ or $v_{i,j}$ by use of the continuity equation with both of the other surface velocities unchanged. The four possibilities are shown in Figs. 10a–d, with the velocity to be assigned indicated in each case. For the situations shown in Figs. 10a and b, the SMAC procedure is the same as the MAC procedure. For the situations of Figs. 10c and d, however, the surface velocity assigned by the SMAC procedure is not

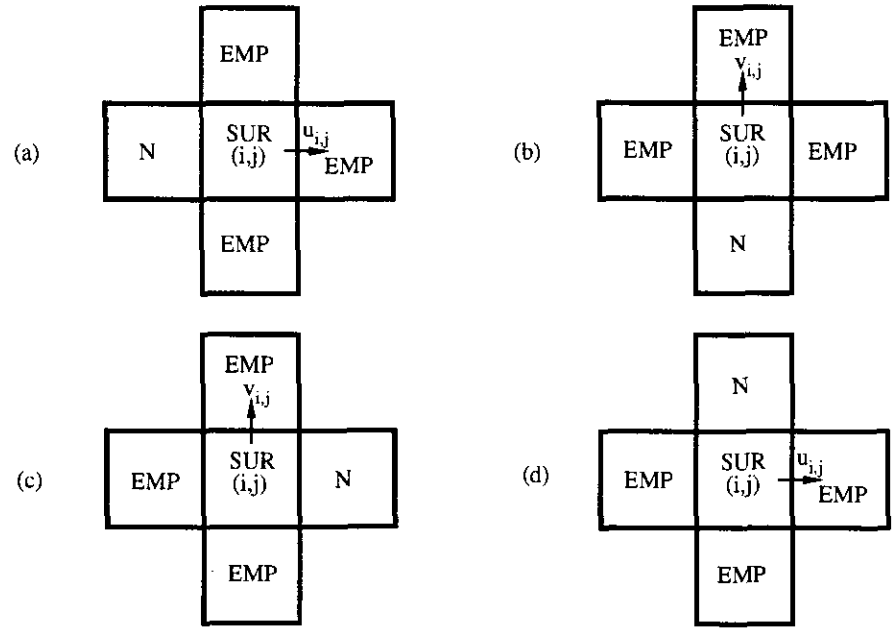

FIG. 10. The surface velocity assigned in the SMAC method for a surface cell with three empty neighbors (N = non-empty).

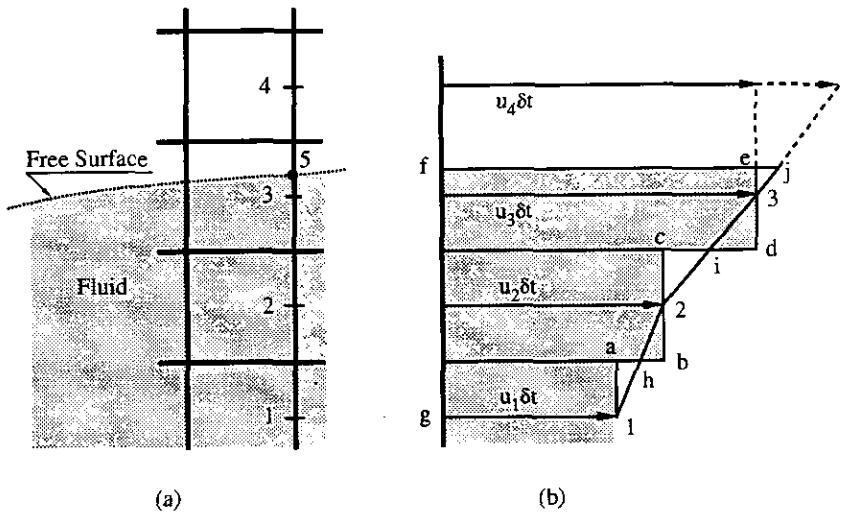

FIG. 11. Just outside tangential velocity assignment and mass transfer.

the same one assigned by the MAC procedure, and use of the SMAC procedure for either of these two situations will artificially introduce asymmetry into the velocity field.

5. JUST OUTSIDE TANGENTIAL VELOCITIES

Referring again to Fig. 4, a velocity such as $v_{i,j}$ that is associated with a face between two empty cells which themselves are adjacent to surface cells is termed a just outside tangential velocity. Like surface velocities, just outside tangential velocities must also be determined in both Steps 5 and 7 of each computational cycle. The just outside tangential velocities assigned in Step 5 influence the movement of markers that occurs in Step 6, while those assigned in Step 7 provide boundary conditions for the calculation of the tentative internal velocities in the next computational cycle.

Previous procedures for the assignment of just ouside tangential velocities only satisfy very roughly the free surface tangential stress condition. In addition, the tangential stress condition itself applies only at the free surface, while the velocities employed in an attempt to satisfy it are separated by the width of a cell. Therefore, an entirely different rationale for the assignment of just outside tangential velocities is used in the new method. The rationale used is that a just outside tangential velocity must be assigned in such a way that the implied mass transfer across the face between the related surface cells is neither exaggerated nor reduced.

The rationale supporting the new just outside tangential velocity assignment procedure is explained with reference to Fig. 11. Since the control volume concept is adopted in the development of the numerical representations of the governing equations, the velocity located at the center of a cell face represents the average fluid velocity on that cell face. Consider Fig. 11a, where points 1, 2, 3, and 4 represent the mid-points of the faces of four cells, and point 5 represents the intersection of a free surface with the face of one of these cells. In Fig. 11b, u_1, u_2, and u_3 represent the average velocities on their respective cell faces. Therefore, the area enclosed by lines connecting points 1–*a*–*b*–*c*–*d*–*e*–*f*–*g*–1 represents the volume of fluid ΔV passed through line segments 1–2–3–5 during a time interval δt. Now, if one imagines a vertical column of markers that coincides with the right faces of the cells shown in Fig. 11a, then the velocity assigned to any one of these markers for marker movement would simply be determined by linear interpolation between the discrete velocities above and below the marker in question. The volume of fluid ΔV_1 passed through the faces of these cells during the time interval δt that is implied by these marker velocities is represented by the area 1–*h*–2–*i*–3–j–e–f–g–1. The area 3–*j*–*e*–3 represents the difference between ΔV and ΔV_1. Consequently, the mass transfer through the right face of the control volume of the surface cell that is implied by the marker velocity assignment scheme is larger (since u_4 is greater than u_3) than that which occurs if u_3 is treated as the average velocity on the right face of the control volume. In order to eliminate this difference, the just outside tangential velocity u_4 must be set equal to the value of the nearest internal velocity u_3. This is the procedure used in the new method.

Although the rationale is completely different, the resulting new just outside tangential velocity assignment procedure is similar to the one used in the original MAC method. If any other scheme is used, including the SMAC scheme, the mass transfer through the control volume that coincides with the surface cell that is implied by the marker velocity assignment scheme will be either more or less than the mass transfer that is implied by treating the discrete velocity associated with the center of the cell face as the average velocity for that face. The new treatment of just outside tangential velocities differs from

the MAC treatment in one important respect. The MAC treatment of just outside tangential velocities can lead to asymmetries when fluid surfaces are coming together. This problem is avoided in the new method; in contrast with either the MAC or SMAC method, just outside tangential velocities are assigned and used only when needed. They are not stored; only surface and internal velocities are stored. Therefore, when two fluid fronts approach each other, the just outside tangential velocity between them will be assigned the value of one internal velocity when the boundary condition associated with one of the converging fluid fronts is under consideration, and the value of a different internal velocity when the boundary condition associated with the other fluid front is under consideration. This is a subtle, but very important, point. The just outside tangential velocity that is stored in either the MAC or SMAC method is used as a boundary condition in the computations of the velocities of the markers and the tentative internal velocities associated with both fluid fronts, despite the fact that it is only related to the motion of one of the two fluid fronts. It is entirely unrelated to the motion of the other fluid front and, therefore, inappropriate for use as a boundary condition for that fluid front. This shortcoming of the MAC and SMAC assignment procedures may be even more important than the fact that they both also artificially introduce asymmetry.

6. NUMERICAL EXAMPLES

Four examples are presented to illustrate the importance of the procedures used for the assignment of free surface velocity boundary conditions in the simulation of free surface fluid flow. The first example illustrates the fact that previous procedures for the assignment of free surface velocity boundary conditions artificially introduce asymmetry. Two cavity filling examples and a broken dam example demonstrate the significant improvements achieved by use of the more accurate new free surface velocity boundary conditions presented in this paper. In all examples, the solutions are illustrated by figures that indicate the fluid-filled regions at specific times. Thick solid lines represent rigid boundaries, thin dotted lines indicate the computational grid, and dots represent markers.

6.1. *Illustration of Asymmetry*

To dramatically illustrate the fact that the SMAC procedures for the assignment of free surface boundary conditions artificially introduce asymmetry, it is demonstrated that there are actually *four* different SMAC solutions for half of any symmetrical problem. If one half of the problem is simulated, one solution is obtained. If the other half of the problem is simulated, a second solution is obtained. If the complete symmetrical problem is simulated, the left and right halves of the complete solution represent third and fourth solutions. As a direct result of the fact that some of the SMAC free surface velocity boundary condition assignment procedures are inherently asymmetrical, all four solutions are different.

In Fig. 12, different SMAC solutions at time $t = 16$ s of a symmetrical cavity-filling problem are presented. At $t = 0$ s, fluid began to enter the cavity from below with a constant velocity. The solutions of the left half of the problem, the right half of the problem, and the complete problem are shown. Since the problem itself is symmetrical, the solutions of the left and right halves of the problem should be mirror images of each other, and they should be identical to the left and right halves, respectively, of the solution of the complete problem. Careful inspection of Fig. 12 reveals, however, that this is not the case. Instead, Figs. 12a and b reveal that the solutions of the left and right halves of the problem are not mirror images of each other; Fig. 12c reveals that the left half of the complete solution is not the mirror image of the right half of the complete solution; and comparison of Figs. 12a and b with Fig. 12c reveals that the solutions of the left and right halves of the problem are not even the same as the left and right halves, respectively, of the solution of the complete problem. As explained in preceding sections and demonstrated in the following examples, this fundamental problem is eliminated by use of the new procedures for the assignment of free surface velocity boundary conditions.

6.2. *First Cavity-Filling Example*

For this example, fluid enters the cavity with a uniform vertical velocity of $U = 1$ cm/s through a gate in the center of the bottom side of the cavity. The cavity is 10 by 7.5 cm and the cell dimensions δx and δy are both equal to 0.5 cm, resulting in a computational domain that is 20 cells by 15 cells. The gate width is six cells (3 cm). The values used for the acceleration of gravity and the kinematic viscosity of the fluid are $g = 1$ cm/s^2 and $\nu = 0.2$ cm^2/s, respectively. This is a perfectly symmetrical problem. The parameter values used for this example are exactly the same as those used to obtain the solutions shown in Fig. 12.

Three solutions of this symmetrical problem are shown in Fig. 13. For this example, the SM method [8] is essentially an efficient version of the SMAC method. The SM method employs only one string of markers along the free surface and requires only the reflagging of the cells along and adjacent to the free surface. The SM method, therefore, requires considerably less computer time and memory than the SMAC method. In other respects, however, especially including the procedures for the assignment of free surface velocity boundary conditions, the SM method is identical to the SMAC method. The SM method modified by the incorporation of the new free surface velocity boundary conditions presented in this paper is referred to here as the VELBC method. Comparisons between VELBC results and either SMAC or SM results illustrate the significance of the use of the new free surface velocity boundary conditions.

In the illustrations of SMAC solutions, markers are distributed throughout the fluid-filled region, whereas a single string of markers surrounds the fluid-filled region in the illustrations of SM and VELBC solutions. Sixteen markers are initially

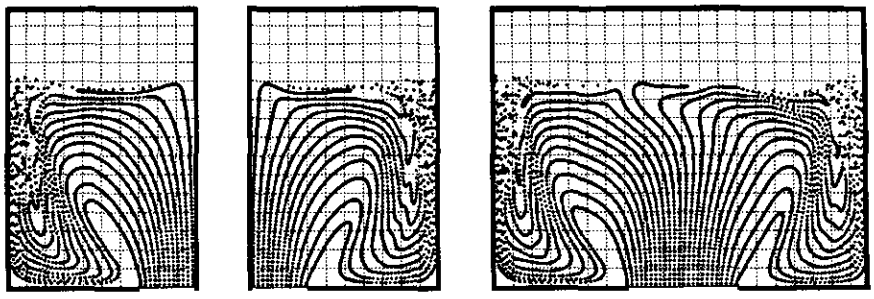

FIG. 12. Illustration of asymmetry in SMAC solutions of a cavity filling problem (g = 1 cm/s^2, ν = 0.2 cm^2/s, U = 1 cm/s, t = 16 s).

assigned to each fluid-filled cell in the SMAC simulation, and the maximum distance between consecutive surface markers is $\delta x/4$ in the SM and VELBC simulations. Consequently, the distance between adjacent markers is initially the same (1.25 mm) in all three simulations.

Inspection of Fig. 13 reveals that the SMAC solution of this symmetrical problem immediately becomes asymmetrical and remains so. This artificially induced asymmetry is caused by the free surface velocity boundary conditions that are employed in the SMAC method.

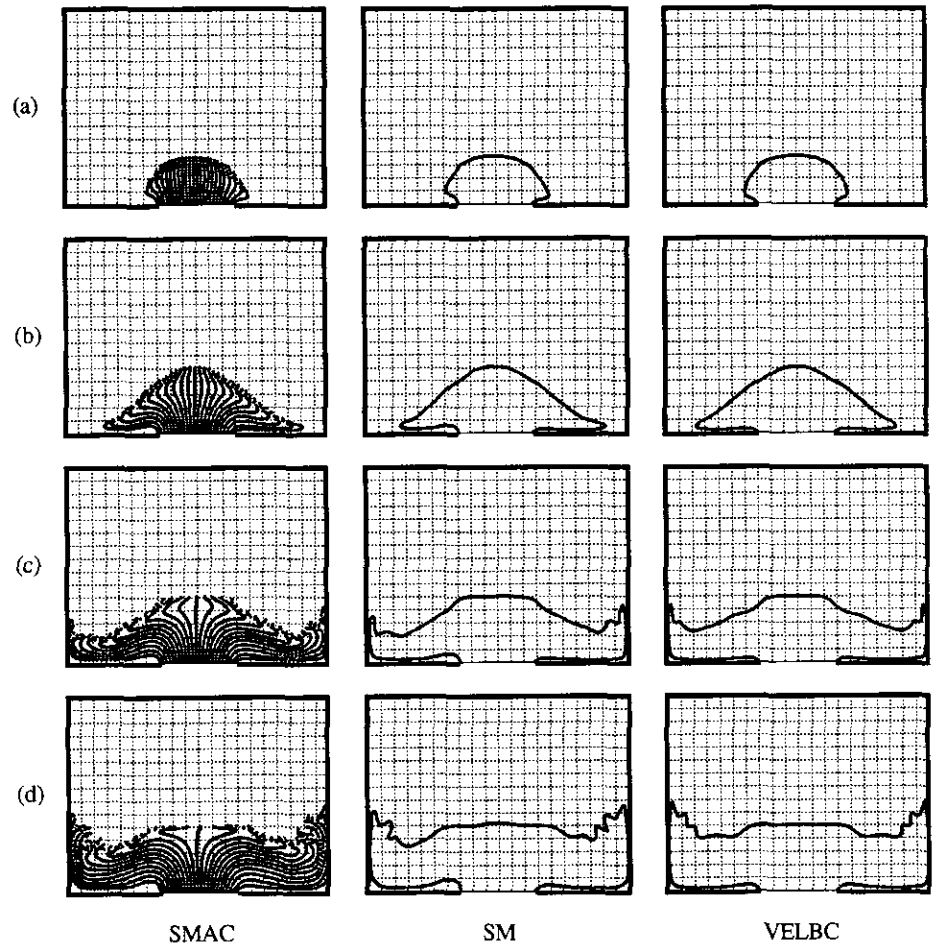

FIG. 13. SMAC, SM, and VELBC solutions of the first cavity filling problem with g = 1 cm/s^2, ν = 0.2 cm^2/s, U = 1 cm/s, and δt = 0.01 s at (a) 2 s, (b) 4 s, (c) 6 s, and (d) 8 s.

The SM solution shown in Fig. 13 faithfully reproduces the SMAC results, including the asymmetries. In Ref. [8] a number of additional examples are presented which also demonstrate that the SM method, although far more efficient than the SMAC method, produces results that are equivalent to those obtained by use of SMAC. As shown in the next example, however, this equivalence between SMAC and SM results exists only if the markers in the SMAC simulation do not become too sparse for the cells to be flagged correctly.

The VELBC results shown in Fig. 13 demonstrate that the replacement of the SMAC free surface velocity boundary conditions with the new conditions eliminates the asymmetries that are present in the SMAC and SM results. The only difference between the VELBC method and the SM method is that the new procedures for the assignment of free surface velocity boundary conditions are used in the VELBC method in lieu of the SMAC procedures which are used in the SM method. As a direct result of the use of the new free surface velocity boundary conditions, the flow pattern associated with the VELBC solution shown in Fig. 13 is symmetrical, as it should be for this symmetrical problem.

6.3. *Second Cavity-Filling Example*

The only difference between this example and the previous example is that the value of the kinematic viscosity is much smaller in this example. The kinematic viscosity in this example is 0.01 cm^2/s, which is appropriate for water at room temperature, whereas the value used in the first example is an order of magnitude larger (0.2 cm^2/s).

The SMAC, SM, and VELBC results for this symmetrical problem are displayed in Fig. 14. As in the first cavity-filling example, the SMAC solution is asymmetrical soon after the fluid enters the cavity. In contrast with the first example, however, the SMAC solution of this second cavity-filling example breaks up as shown in Figs. 14c and d. The breakup of the SMAC solution is due both to the deficiencies of the SMAC procedures for the assignment of free surface velocity boundary conditions as well as to reflagging errors that occur in a SMAC simulation when the markers become too sparse for the cells to be reflagged correctly. This difficulty associated with the use of markers in the MAC or SMAC method has been referred to in Refs. [4, 8]. In the first cavity-filling example, the viscosity is one order of magnitude larger, and the markers do not become too sparse in the SMAC simulation.

Since the SMAC solution breaks up, the SM solution shown in Fig. 14 for this example does not reproduce the SMAC results. The differences between the SMAC and SM results for this example are due to the fact that the spacing between surface markers is managed in the SM method. Specifically, in the SM method, a new marker is added midway between two adjacent surface markers when the distance between the markers exceeds a predetermined value. The ability to add surface markers is an important additional advantage of the SM method. The problems that arise during a SMAC simulation simply because the markers become too sparse in a certain region for proper reflagging to occur are eliminated in the SM method. It is especially important to note, however, that the elimination of the SMAC reflagging problems by use instead of the SM method does not eliminate all of the difficulties associated with the simulation of this problem. The SM solution shown in Fig. 14 is asymmetrical and clearly not a valid solution. The very unusual shape of the free surface in the SM solution is a clear indication that incorrect velocities exist. The problems manifested in the SM solution of this example have nothing to do with the use of surface markers in lieu of markers distributed throughout the fluid. Instead, they are due to the use in the SM method of the SMAC procedures for the assignment of free surface velocity boundary conditions.

The VELBC results shown in Fig. 14 demonstrate the dramatic effect on the solution for this problem of the replacement of the SMAC free surface velocity boundary conditions with the new free surface velocity boundary conditions. The VELBC solution for this problem is symmetrical, as it should be, and, most importantly, it does not exhibit the breakup exhibited by the SMAC solution.

Comparison of the SM and SMAC results shown in Fig. 14 reveals the effect of the elimination of the reflagging difficulties associated with the use of the SMAC method. Subsequent comparison of the VELBC results with the SM results then reveals the additional effect of the use of the new free surface velocity boundary conditions. The combined effect of the use of the new free surface velocity boundary conditions and of surface markers is illustrated by the dramatic difference between the VELBC and SMAC results shown in Fig. 14.

It may be somewhat surprising that changes in the treatment of the free surface velocity boundary conditions can have such a dramatic effect on the simulation. The free surface velocity boundary conditions, however, affect every aspect of the simulation. The tentative velocity field is directly affected by the free surface velocity boundary conditions. The tentative velocity field in turn directly affects the pressure potential field. Then, the final velocities are computed from the tentative velocity and pressure potential fields. Next, free surface velocity boundary conditions must be assigned, and they then directly affect the movement of the free surface. After the advance of the free surface, free surface velocity boundary conditions must be adjusted, including the assignment of any unknown new fluid cell internal velocities. These free surface velocity boundary conditions subsequently directly affect the determination of the tentative velocity field in the next computational cycle and so on.

If, instead of decreasing the value of the kinematic viscosity of the fluid as compared with the value used in the first cavity-filling example, the value of the acceleration of gravity is increased, results similar to those shown in Fig. 14 are obtained. That is, the SMAC solution exhibits breakup in addition to asymmetry, while the new VELBC solution is symmetrical

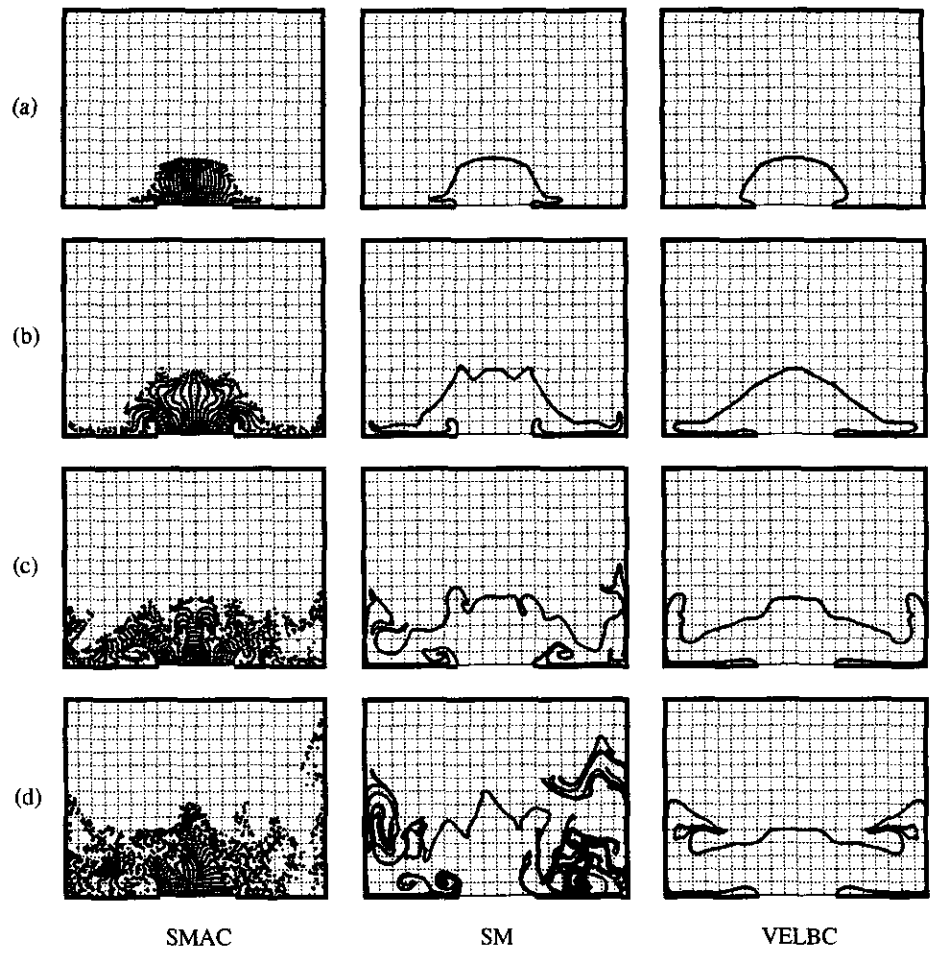

FIG. 14. *SMAC, SM, and VELBC solutions of the second cavity filling problem with* $g = 1$ cm/s^2, $\nu = 0.01$ cm^2/s, $U = 1$ cm/s, and $\delta t = 0.01$ s at (a) 2 s, (b) 4 s, (c) 6 s, and (d) 8 s.

with no breakup. With the use of the new free surface velocity boundary conditions, realistic values of g and ν can be accommodated without difficulty. This is a very important point. The new free surface velocity boundary conditions fundamentally affect the simulation. They eliminate asymmetry, and they also have a very significant effect on the range of application of the simulation method itself.

6.4. *Broken Dam Example*

To further emphasize the fact that the significance of the new procedures is not limited to the elimination of asymmetry, a broken dam example is presented. The broken dam problem is not a symmetrical problem. The SMAC and VELBC results for this problem are presented in Fig. 15. In the broken dam problem, a vertical fluid column located in the lower left section of the computational region is initially at rest. Gravity acts downward, and nothing constrains the fluid on the right side of the fluid column. Consequently, the fluid immediately begins to flow down and to the right as shown in Figs. 15a–c. The dimensions of the initial fluid column are 10 cells by 10 cells (5 by 5 cm). The value used for g is 980 cm/s^2, which is appropriate for the Earth, and the value used for ν is 0.01 cm^2/s, which is appropriate for water at room temperature.

As shown in Figs. 15d–f, the SMAC simulation breaks up when these realistic values of g and ν are used. As discussed in connection with the previous example, this breakup of the SMAC solution is related both to the deficiencies of the SMAC procedures for the assignment of free surface velocity boundary conditions as well as to reflagging errors that occur in the SMAC simulation when the markers become too sparse for the cells to be reflagged correctly. Since surface tension is not modeled in any of the simulation methods under consideration, the breakup of a real fluid that can occur after striking a solid boundary cannot be simulated properly by any of the methods. The breakup displayed in Figs. 15d–f is a numerical artifact. If the SMAC simulation is allowed to continue past the time associated with Fig. 15f, the markers become scattered throughout the computational region. As noted, it is possible for markers in the SMAC solution to become too sparse for all cells along the surface to be flagged correctly. To investigate the possibility that this could be the cause of the breakup shown in Fig. 15,

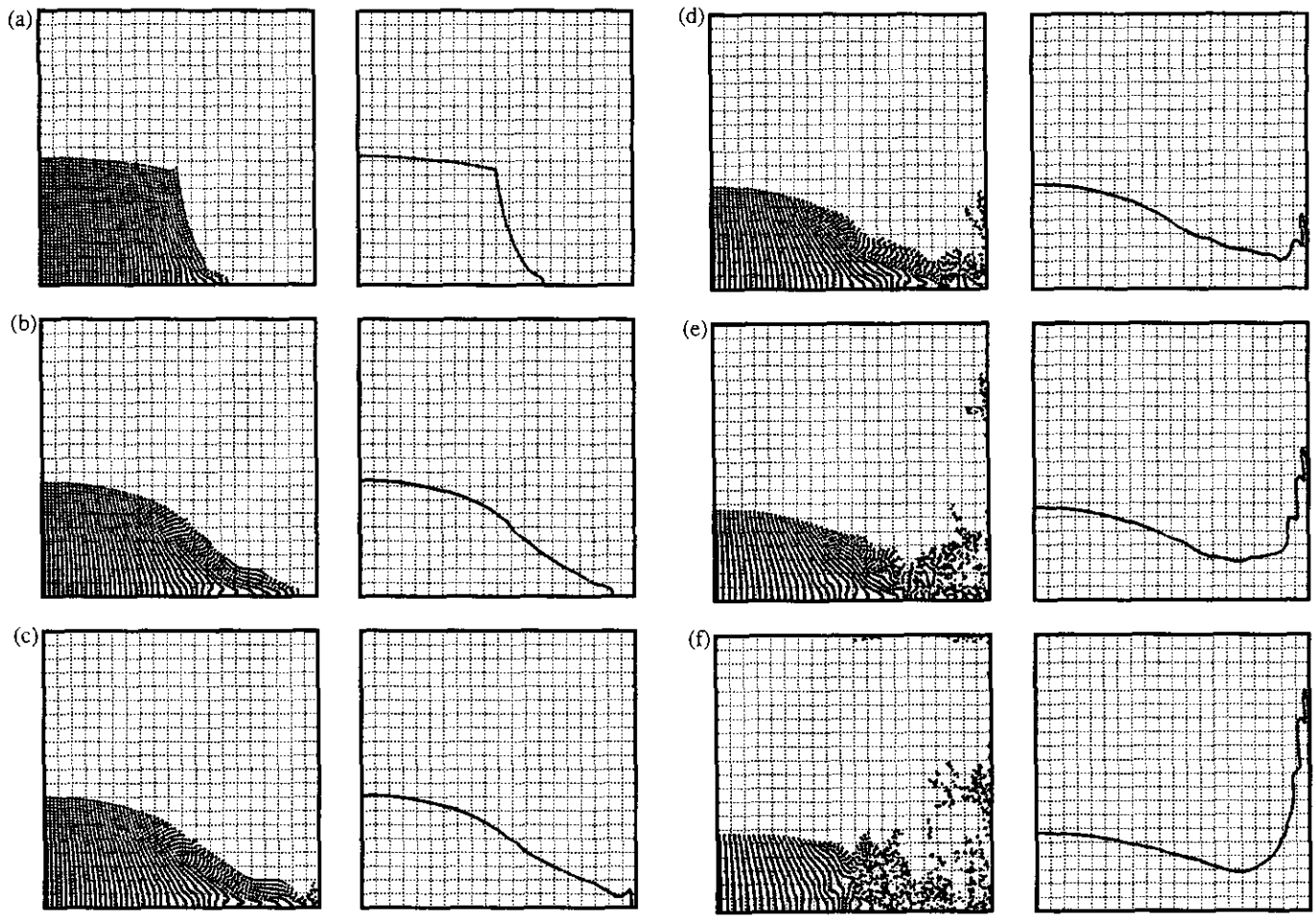

FIG. 15. SMAC and VELBC solutions of the broken dam problem with $g = 980$ cm/s^2, $\nu = 0.01$ cm^2/s, and $\delta t = 0.0002$ s at (a) 0.042 s, (b) 0.072 s, (c) 0.080 s, (d) 0.096 s, (e) 0.120 s, and (f) 0.148 s.

another SMAC simulation of the same problem was conducted using a greatly increased number of markers, 64 per cell, rather than 16 per cell. Breakup also occurred in this second SMAC simulation. The use of more markers simply altered the specific details of the breakup.

In this example, as well as in the previous one, the use of the new free surface velocity boundary conditions and of surface markers effectively eliminates the breakup and enables the new VELBC simulation to accommodate without difficulty the realistically high and low values of g and ν, respectively. The dramatic differences between the SMAC and VELBC results for this asymmetrical problem add emphasis to the fact that the significance of the fundamental contributions to the treatment of free surface velocity boundary conditions extends beyond the elimination of artificially induced asymmetry.

7. CONCLUSIONS

Free surface velocity boundary conditions play a critical role in the simulation of fluid flow problems involving free surfaces. New, more accurate procedures for the application of free surface velocity boundary conditions are presented in this paper. The significant advantages of the use of these new procedures are demonstrated by examples.

A useful tangible indicator of the accuracy of the application of free surface velocity boundary conditions is the symmetry of the solution of a symmetrical problem. It is shown that previous procedures for the application of free surface velocity boundary conditions artificially introduce asymmetry. No asymmetry is introduced by use of the new procedures.

More importantly, it is shown that, in addition to the elimination of asymmetry, the use of the new procedures extends the range of application of the simulation method. When previous procedures for the application of free surface velocity boundary conditions are used, it is observed that the solution breaks up when realistically low values of viscosity and/or realistically high values of gravity are used. However, solutions without breakup are obtained simply by replacing the previous procedures for the application of free surface velocity boundary conditions with the new procedures presented in this paper.

ACKNOWLEDGMENTS

Support for this research has been provided by the Defense Advanced Research Projects Agency of the U.S. Department of Defense as Projects 5-25084 and 5-25085 of Contract MDA093-86-C-0182, the National Science Foundation under Grant DDM-9114846, and the Leadwell CNC Machines Manufacturing Corporation.

REFERENCES

1. A. A. Amsden, Los Alamos Scientific Laboratory Report LA-5146, 1973 (unpublished).
2. A. A. Amsden and F. H. Harlow, Los Alamos Scientific Laboratory Report LA-4370, 1970 (unpublished).
3. A. A. Amsden and F. H. Harlow, *J. Comput. Phys.* **6,** 322 (1970).
4. N. Ashgriz and J. Y. Poo, *J. Comput. Phys.* **93,** 449 (1991).
5. U. Bulgarelli, V. Casulli, and D. Greenspan, "Pressure Methods for the Numerical Solutions of Free Surface Fluid Flows," (Pineridge Press, Swansea, UK, 1984).
6. R. K.-C. Chan and R. L. Street, *J. Comput. Phys.* **6,** 68 (1970).
7. R. K.-C. Chan, R. L. Street, and J. E. Fromm, "The Digital Simulation of Water Waves—An Evaluation of SUMMAC," in *Proceedings, Second International Conference on Numerical Methods in Fluid Dynamics, Berkeley,* (Springer-Verlag, New York/Berlin, 1970), p. 429.
8. S. Chen, D. B. Johnson, and P. E. Raad, *Computational Modelling of Free and Moving Boundary Problems,* Vol. 1, *Fluid Flow* (de Gruyter, New York, 1991), p. 223.
9. F. H. Harlow and J. E. Welch, *Phys. Fluids* **8,** 2182 (1965).
10. C. W. Hirt and J. L. Cook, *J. Comput. Phys.* **10,** 324 (1972).
11. C. W. Hirt, J. L. Cook, and T. D. Butler, *J. Comput. Phys.* **5,** 103 (1970).
12. C. W. Hirt and B. D. Nichols, *J. Comput. Phys.* **39,** 201 (1981).
13. C. W. Hirt, B. D. Nichols, and N. C. Romero, "SOLA—A Numerical Solution Algorithm for Transient Fluid Flows," Los Alamos Scientific Laboratory Report LA-5842, 1975 (unpublished).
14. C. W. Hirt and J. P. Shannon, *J. Comput. Phys.* **2,** 403 (1968).
15. W. S. Hwang and R. A. Stoehr, "Computer Aided Fluid Flow Analysis of The Filling of Casting Systems," in *Proceedings NUMIFORM '86 Conference, Gothenburg, 1986,* p. 361.
16. R. W. Lardner and Y. Song, *Int. J. Numer. Methods Fluids* **14,** 109 (1992).
17. C. Y. Loh and H. Rasmussen, *Appl. Numer. Math.* **3,** 479 (1987).
18. P. I. Nakayama and N. C. Romero, *J. Comput. Phys.* **8,** 230 (1971).
19. B. D. Nichols and C. W. Hirt, *J. Comput. Phys.* **8,** 434 (1971).
20. B. D. Nichols and C. W. Hirt, *J. Comput. Phys.* **12,** 234 (1973).
21. B. D. Nichols, C. W. Hirt, and R. S. Hotchkiss, "SOLA-VOF: A Solution Algorithm for Transient Fluid Flow with Multiple Free Boundaries," Los Alamos Scientific Laboratory Report LA-8355, *1980* (unpublished).
22. M. D. Torrey, L. D. Cloutman, R. C. Mjolsness, and C. W. Hirt, "NASA-VOF2D: A Computer Program for Incompressible Flows with Free Surfaces," Los Alamos National Laboratory Report LA-10612-MS, 1985 (unpublished).
23. J. A. Viecelli, *J. Comput. Phys.* **4,** 543 (1969).
24. J. A. Viecelli, *J. Comput. Phys.* **8,** 119 (1971).
25. J. E. Welch, F. H. Harlow, J. P. Shannon, and B. J. Daly, Los Alamos Scientific Laboratory Report LA-3425, (unpublished).